Communication: Influence of external static and alternating electric fields on water from long-time non-equilibrium ab initio molecular dynamics

Zdenek Futera, and Niall J. English

Citation: The Journal of Chemical Physics **147**, 031102 (2017);
View online: https://doi.org/10.1063/1.4994694
View Table of Contents: http://aip.scitation.org/toc/jcp/147/3
Published by the American Institute of Physics

Communication: Influence of external static and alternating electric fields on water from long-time non-equilibrium *ab initio* molecular dynamics

Zdenek Futera[a),b)] and Niall J. English[a)]
School of Chemical and Bioprocess Engineering, University College Dublin, Belfield Dublin 4, Ireland

(Received 1 May 2017; accepted 6 July 2017; published online 21 July 2017)

The response of water to externally applied electric fields is of central relevance in the modern world, where many extraneous electric fields are ubiquitous. Historically, the application of external fields in non-equilibrium molecular dynamics has been restricted, by and large, to relatively inexpensive, more or less sophisticated, empirical models. Here, we report long-time non-equilibrium *ab initio* molecular dynamics in both static and oscillating (time-dependent) external electric fields, therefore opening up a new vista in rigorous studies of electric-field effects on dynamical systems with the full arsenal of electronic-structure methods. In so doing, we apply this to liquid water with state-of-the-art non-local treatment of dispersion, and we compute a range of field effects on structural and dynamical properties, such as diffusivities and hydrogen-bond kinetics. *Published by AIP Publishing.* [http://dx.doi.org/10.1063/1.4994694]

The distinctive, and sometimes puzzling, properties of water are thought to depend fundamentally on the microscopic characteristics and nature of hydrogen bonding.[1] Indeed, hydrogen-bond formation and breakage govern the dynamical behaviour of liquid water.[2] The resulting intrinsic electric fields in condensed phases of water have been estimated by molecular dynamics (MD) at ∼1.5 to 2.5 V/Å.[3] The response of water to externally applied electric fields is of central relevance in the modern world, where many extraneous electric fields are ubiquitous. The effects of external electric fields, both time-varying [e.g., oscillating and cosine-varying, the dominant component of electromagnetic (e/m) fields] and static, on liquid water have been simulated by non-equilibrium (NE-) MD.[4–9] It has been found that a general linear-response régime[10] is in the vicinity of field intensities up to ∼0.05 V/Å,[5–7] in that external-field forces and torques are no more than a few percent of those present intrinsically due to electrostatic fields created by intermolecular charge distributions.

Historically, the application of external fields in non-equilibrium MD has been restricted to relatively inexpensive empirical models, varying in sophistication of the treatment of polarisability. Given that applied-field intensities have often been of the order of 0.1 V/Å, so as to discern tangible field effects within accessible simulation time scales of tens of picoseconds or longer, this presents somewhat of a quandary: the dielectric-saturation threshold of water, for instance, is ∼0.006 V/Å, and widely used empirical models do not typically allow for molecular dissociation. Indeed, "simplistic" models of water do not handle induced electronic polarisation following electric-field application and/or removal, as electron-cloud dynamics occurring orders of magnitude faster than nuclear dynamics is neglected. Even more sophisticated polarisable empirical water models[11] do not allow for a rigorous view on electronic-structure reorganisation in external electric fields and only capture this approximately,[4,5] disregarding molecular dissociation. Therefore, non-equilibrium *ab initio* MD (NE-AIMD) is needed to capture more subtle electronic-structure effects in external electric fields. To that end, Umari and Pasquarello pioneered ground-state NE-AIMD in external electric fields via the rigorous Berry-phase approach under periodic boundary conditions (PBC) for Density Functional Theory (DFT)-based Car–Parrinello (CP) dynamics, for bulk MgO.[12] Saitta *et al.*[13] performed non-deterministic CP-MD coupled with transition-path sampling, to study liquid water and its break-up in intense (Berry-phase) static fields, finding a "threshold" dissociation intensity of ∼0.35 V/Å, whilst break-up started to occur above this intensity. Saitta and Saija conducted intriguing *in silico* "Miller experiments" using similar in-field CP-MD and metadynamics treatments to study the formation of formic acid and formamide in aqueous solutions under static fields.[14] In subsequent interesting work, Cassone *et al.* studied, using similar NE-CPMD-based methods, intense (∼0.2 V/Å, and upwards) static-field effects on ice's mechanical/electric properties,[15] liquid methanol,[16] and salty liquid water,[17] typically with a view of determining molecular-dissociation thresholds.

Bearing in mind the need for Berry-phase NE-AIMD treatment of condensed-matter systems' dynamical response to externally applied electric fields, in view of subtleties of electronic-structure rearrangement treated crudely by even sophisticated polarisable empirical models, there exist further compelling methodological advances necessary to allow this avenue of endeavour to progress, despite very encouraging recent progress.[12–17] Specifically, as concluded previously,[9] simulations approaching nanosecond time scales are necessary to reduce "signal-to-noise" ratios of applied

a) Authors to whom correspondence should be addressed: z.futera@ucl.ac.uk and niall.english@ucd.ie. Tel.: +353-1-7161646. Fax: +353-1-7161177.
b) Present address: Department of Physics and Astronomy, University College London, Gower Street, London WC1E 6BT, United Kingdom.

fields and allow for use of more experimentally realistic, lower-intensity, linear-response-régime field intensities with less system-heating problems. A second desideratum is the use of time-varying external fields, e.g., for electromagnetic (e/m)-field exposure.[9] Here, we overcome these fundamental difficulties to report longer-time non-equilibrium *ab initio* molecular dynamics in both static and oscillating electric fields. In so doing, we apply this to liquid water with state-of-the-art non-local treatment of dispersion, computing field effects on structural and dynamical properties, such as diffusivities and hydrogen-bond kinetics. We choose water because of the relatively low energy barriers for dipolar re-orientation leading to greater clarity of argument.[8]

(NE-) AIMD simulations under periodic boundary conditions (PBC) were carried out using the vdW-DF functional with explicit non-local Dion-Rydberg-Schröder-Langreth-Lundqvist (DRSLL) correlation correction describing the van der Waals interaction.[18,19] For the exchange part, the optimized Becke 88 (optB88) Generalised Gradient Approximation (GGA)-type functional was used.[20] This DRSLL approach has been shown recently to perform well for liquid water,[21–26] with optB88-DRSLL arguably being superior.[20] However, due to the still rather over-structured nature of water,[20–26] even from more sophisticated DRSLL-based treatments, it was still found necessary here to run BO-MD at 330 K to capture liquid-state physical behaviour at ~298 K. In order to isolate athermal effects as much as possible, non-equilibrium (N)NVT[3,9] was carried out (at 330 K). Here, a 1 fs time step was used with a density of 0.997 g/cm^3, in conjunction with Langevin stochastic thermostatting.[27,28] The wavefunction was described by the TZV2P basis set with core-electron Goedecker-Teter-Hutter (GTH) pseudopotentials from the CP2K database.

Long 100 ps NE-AIMD trajectories for systems containing 64 water molecules, in the absence and presence of external fields, were obtained via second-generation Car–Parrinello MD,[27,28] using in-house-modified CP2K software. Good structural and dynamical characteristics of water were obtained via second-generation Car–Parrinello MD,[29] e.g., radial distribution functions, self-diffusion coefficients, and vibrational spectra.

Uniform external static and oscillating electric fields were applied with **E** along the laboratory z-direction via the Berry-phase approach,[12] with $\mathbf{E}(t) = E_{Max} \cdot \mathbf{k} \cdot \cos \omega t$ in the case of oscillating fields.[3,4,9] The static-field intensities applied were 0.05 and 0.1 V/Å, whilst r.m.s. intensities for the oscillating fields were set at the same level (and $E_{\max} = \sqrt{2}E_{\mathrm{rms}}$);[3,4,9] frequencies were 50, 100, and 200 GHz. 100 ps is sufficiently long for 50 GHz oscillating fields to have at least 5 applied field 20 ps-period cycles. Generally, in the condensed phase, water has intrinsic electric-field intensities in the range ~1.5-2.5 V/Å,[3] so the external-field torques on each molecule are of the order of 2%-8% of those inherently present due to interaction with neighbouring molecules, affording a reasonable "signal-to-noise" ratio and allowing for transition into the non-linear response regime at 0.1 V/Å.[5,7] As mentioned previously, although applied fields here exceed the dielectric-breakdown threshold, sub-nanosecond simulations are insufficiently long to lead to water dissociation at these applied intensities, and no water dissociation was observed here; indeed, this is by design, as water dissociation *per se* is not the goal of this study.

In terms of intramolecular geometry, there is no particular perturbation from the alternating fields of the averaged O_w–H_w bond length d_{oh}, H_w–O_w–H_w valence angle α_{hoh}, and size of dipole moment μ (cf. Table I), as back-and-forth motion along laboratory $\pm z$ directions leads to net cancellation of any persistent effect. However, in static fields, it is perhaps unsurprising that constant orientation of the field along the laboratory $+z$-direction leads to a partial dipolar alignment therewith; this results in a slight lengthening of d_{oh}, decrease in α_{hoh}, and attendant increase in μ (by about 0.5%-0.8% for each quantity). Such a slight dipolar enhancement has been observed recently in absorbed-water layers at titania surfaces in similar external static fields, via flexible empirical models.[30]

In contrast, perturbation of intermolecular structure is more stark, including via oscillating fields—underscored by site-site radial distribution functions (RDFs) in Fig. 1. Here, the partial dipole alignment afforded by static fields sharpens rather dramatically the first coordination-layer peak (R_{OO} ~ 2.5-3 Å), with concomitant deepening of "trough" at 3-3.5 Å, with more marginal structural accentuation in the second layer (R_{OO} ~ 4-5 Å). Precisely, the opposite ("blurring") effect is seen for oscillating fields (especially at 200 GHz with field periods of only 5 ps). This accentuation of intermolecular (RDF) structure in static fields, and relative loss of definition in alternating ones, arises from time-averaging of greater dipolar alignment in the static case, and, for oscillating fields, over a gamut of field-tracking alternating alignments over a number of applied-field cycles. Similar loss of definition has been seen in liquid-water RDFs in Ref. 3 in electromagnetic fields.

Figure 2 depicts the z-component of molecular dipole moment, μ_z, under zero-, static-, and oscillating-field conditions. As expected, there is no dipole-orientational preference under zero-field conditions, and a strong peak at ~1.4 D in the $+z$-direction in static fields (with overall averaged μ at ~1.475 D in magnitude), indicating increasing dipole alignment (and "locking") with greater field strength.[7–9] In marked contrast, the oscillating fields show maxima at either peak-field extremum along the ±z-directions (i.e., when $E(t) = \pm E_{Max}$), particularly at 50 GHz, where there is greater time with the longer 20 ps field periods allowing greater scope for enhanced partial reorientation in response to the molecular torques

TABLE I. Static properties of bulk water: mean O_w–H_w bond length (d_{oh}), mean H_w–O_w–H_w valence angle (α_{hoh}), and mean molecular dipole moment (μ).

	Intensity (V/Å)	Frequency (GHz)	$\langle d_{oh} \rangle$ (Å)	$\langle \alpha_{hoh} \rangle$ (deg)	$\langle \mu \rangle$ (D)
No field	0.00	0	0.993	105.335	1.465
Static field	0.05	0	0.995	105.040	1.471
	0.10	0	0.998	104.765	1.477
Oscillating field	0.05	50	0.993	105.240	1.467
	0.05	100	0.993	105.320	1.466
	0.05	200	0.993	105.299	1.466
	0.10	50	0.994	104.922	1.475
	0.10	100	0.993	105.065	1.472
	0.10	200	0.993	105.072	1.472

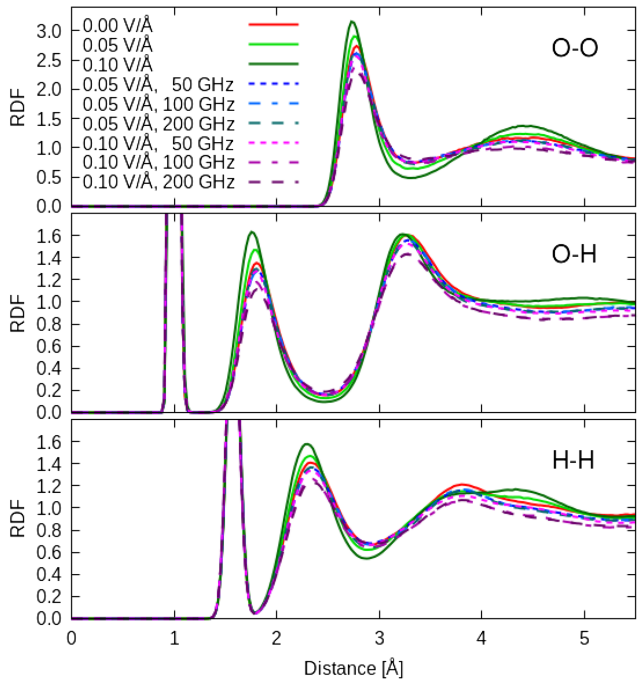

FIG. 1. Radial distribution function (RDF) for O–O, O–H, and H–H pair interactions in bulk water under zero-field conditions (solid red lines), static electric fields (solid green lines), and oscillating electric fields (dashed lines).

acting along the ±z-directions. As is the case with the RDFs in Fig. 1, higher-frequency oscillating fields allow less time for dipole "tracking" of the field direction, resulting in less RDF definition and a more "smeared" z-dipole histogram[3,7] in Fig. 2. The lack of time averaging of the μ_z-distribution shows in vivid detail this sensitivity of dipole response *within* the field cycles, which has thus far been less obvious when considering time-/cycle-*averaged* system- and molecular-response properties.

Consideration of (Luzar-Chandler-defined)[31] hydrogen-bond properties is illuminating. In Fig. S1 (cf. supplementary material), dramatically opposing effects are again clearly evident in the hydrogen-bond acceptor-H distance vis-à-vis zero-field conditions: static fields shorten this somewhat, whilst

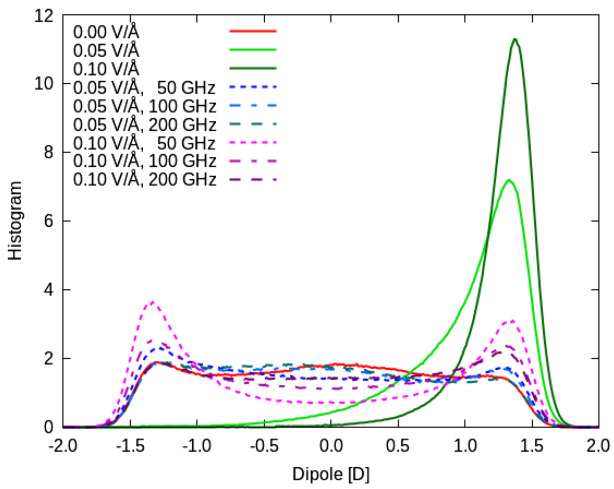

FIG. 2. Distribution of z-component of molecular dipole moments under various field (and zero-field) conditions, with labeling as in Fig. 1.

oscillating fields serve primarily to broaden the distribution, and shift slightly to greater distances. Similar opposite trends are exhibited in Fig. S2 of the supplementary material by the acceptor-donor-hydrogen angle, where the static-field contraction in the A-D-H angle mirrors that of intramolecular angle, at the foot of substantial (z-axis) dipole alignment (cf. Fig. 2); in stark contrast, the torque-induced reduction in hydrogen-bond kinetics leads to greater strain and "loosening" of A-D-H angles towards slightly larger values, but with the primary effect of broadening the distribution (when time-averaged, as here). The stark hydrogen-bond-behaviour dichotomy is emphasised even more greatly by the distribution of the number of hydrogen-bonded neighbours per molecule (cf. Fig. S3 of the supplementary material). Here, static fields, with their comparative suppression of rotational-diffusive motion and "dipole-locking,"[6–8] lead to a marked increase in the number of hydrogen-bonded neighbours, whilst the reduced *de facto* viscosity of faster-rotating molecules in alternating fields (cf. Refs. 3–9) lessens partly instantaneous classification of the number of hydrogen bonds (cf. Fig. S3). In any event, these various time-static hydrogen-bond properties are reflected in Table S1 of the supplementary material, where average lengths, angles, and numbers are specified.

For hydrogen-bond dynamical behaviour, we calculated average lifetimes using Luzar-Chandler autocorrelation-function (ACF) analysis;[31] results are provided in Table II and Fig. S4 of the supplementary material. In previous NEMD analysis of e/m and oscillating fields (with rigid polarisable and fixed-charge empirical models),[3,7] hydrogen bonds were observed to exhibit substantially faster rearrangement kinetics, as induced dipolar rotations lead to lower viscosity and larger diffusivity. Here, our markedly faster ACF decay experienced in oscillating fields (cf. Fig. S4) is perfectly consistent with this picture;[3,7] however, the dramatic static-field-mediated hydrogen-bond-kinetics slowdown (in the guise of retarded ACF decay in Fig. S4) and the resultant increase in lifetime (Table II), especially well into the non-linear response regime[5,7] at 0.1 V/Å, underscore this static/oscillating bifurcation and agree with previous observations of dynamical retardation in static fields.[8]

In terms of water field-induced roto-translational coupling,[6] we observed parallel inhibition and promotion of

TABLE II. Dynamical properties of bulk water: self-diffusion constant, D, and mean hydrogen-bond lifetime, τ, fitted to the Luzar-Chandler ACFs of Fig. S4 of the supplementary material.

	Intensity (V/Å)	Frequency (GHz)	D (10^{-9} m^2/s)	τ (ps)
Zero field	0.00	0	1.55	2.16
Static field	0.05	0	1.11	2.47
	0.10	0	0.81	3.13
Oscillating field	0.05	50	1.97	2.13
	0.05	100	1.72	2.26
	0.05	200	2.11	2.14
	0.10	50	2.17	2.39
	0.10	100	2.75	2.39
	0.10	200	3.03	1.99

self-diffusivity vis-à-vis the zero-field case by static and alternating fields, respectively (cf. Fig. S5 of the supplementary material and Table II); the oscillating-field results mirror earlier (polarisable) empirical-potential findings of e/m-field-mediated increases in self-diffusivity.[3,5] The lower/higher viscosity of more rapidly/slowly rotating water molecules, respectively, in the respective alternating and static "dipole-locked" fields leads to different mean-squared displacements, and limiting slopes from the Einstein relationship (Fig. S5 of the supplementary material);[32,33] the lower diffusivity values in Table II reflect previous static-field dynamical-retardation findings.[8] To study more closely the subtleties of field-water dynamical (roto-translation) coupling in the local molecular frame, as opposed to laboratory-axis perspectives,[34] Fig. 3 depicts ACFs of internal water-molecule axes along the dipole, H–H, and out-of-plane directions;[35,36] in particular, dipole- and H–H- direction ACFs' decay is related to Debye and NMR relaxation times.[34] Again, the two-way static/oscillating paradigm is starkly evident with retardation and acceleration of ACF decay of all three quantities by static and alternating fields. For alternating fields, 200 GHz leads to the greatest acceleration: here, the 5 ps field period overlaps most closely, compared to 10 and 20 ps for 50 and 100 GHz[3] with ambient-temperature values of Debye, NMR, and hydrogen-bond relaxation times.[5,34,37]

In contrast to empirical potentials, the *ab initio* MD approach allows for the variation in intramolecular-stretch modes without reference to any (an)harmonic "pre-calibrated spring-like" (zero-field) settings, even though more sophisticated empirical models exist to account for changing condensed-phase environment, and do well for IR analysis.[38,39] In any event, a more rigorous quantum-level treatment of external-electric-field perturbation, relative to classical field coupling to empirical potentials, is an important desideratum of Berry-phase-facilitated AI-MD. In Fig. S6 of the supplementary material, we show the computed IR spectrum[30,40] under zero-field conditions, alongside experimental

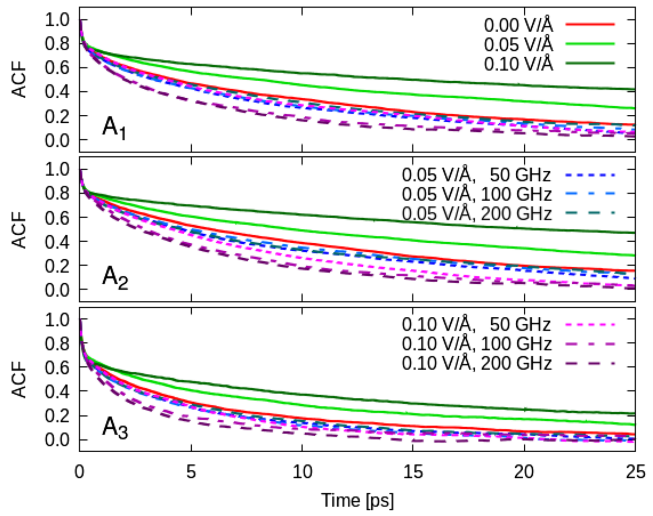

FIG. 3. Autocorrelation functions (ACFs) of internal water-molecule axes: (1) dipole direction $\mathbf{a}_1$, (2) H–H direction $\mathbf{a}_2$, (3) out-of-plane direction perpendicular to $\mathbf{a}_1$ and $\mathbf{a}_2$, i.e., $\mathbf{a}_3 = \mathbf{a}_1 \times \mathbf{a}_2$. Zero-field conditions are denoted by solid red lines, static fields by solid green lines, and oscillating fields by dashed lines.

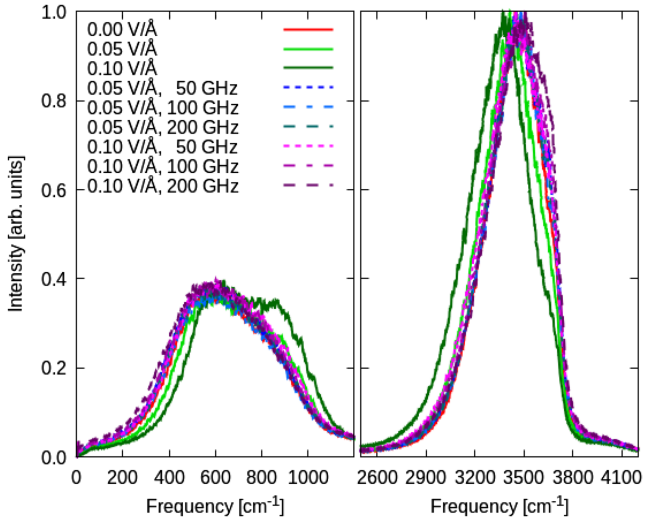

FIG. 4. Effect of static and oscillating electric fields on the librational (left) and vibrational (right) bands of bulk water's IR spectrum; labeling as in Fig. 1.

values at 298 K,[41] as well as in-field spectra in Fig. 4. The agreement between the computed and experimental spectra is semi-quantitative and allows for relative confidence in gauging external-field effects on IR bands in a rigorous Berry-phase manner without any fear of "pre-calibration" as can typically be the case with empirical potentials. In any event, Fig. 4 reinforces the by-now-familiar static-/oscillating-field dichotomy, albeit in an intriguing way: static fields red- and blue-shift vibrational and librational modes, respectively, and vice versa for alternating fields. In the case of librations (rotation oscillations),[36] static fields inhibit gross rotational motion (via partial "dipole locking") and so increase the frequency of the underlying oscillations (i.e., librations *per se*), with alternating fields inducing the opposite effect. Again, the 200 GHz field induces the largest effect in Fig. 4 on the IR bands, due to the optimal 5 ps field-period overlap with underlying ambient-temperature rotational and dipole relaxation times.

In closing, non-equilibrium AI-MD in both static and oscillating external electric fields was carried out within the Berry-phase framework using second-generation Car–Parrinello MD; this opens up rigorous, long-time studies of electric-field effects with electronic-structure methods. For liquid water, we have identified a dichotomy in static- versus oscillating-field response, in that static fields induce dynamical suppression and mechanistic "dipolar locking" and resultant structural RDF-sharpening, with the exact opposite being a feature alternating fields with more-rapidly rotating (and, via roto-translation coupling, translating) water molecules. The hydrogen-bond-rearrangement kinetics also shows this contrasting behaviour of slowdown and acceleration in respective static and alternating fields, with IR spectra showing opposite blue- and red-shifting trends in the librational and vibrational bands.

See supplementary material for static hydrogen-bond properties (distributions of bond lengths, angles, bond numbers, and their mean values), hydrogen-bond autocorrelation functions, mean square displacement curves, and comparison of calculated and experimental IR spectra.

The authors thank Science Foundation Ireland for funding under Grant No. SFI 15/ERC-I3142.

[1]D. Eisenberg and W. Kauzmann, *The Structure and Properties of Water* (Oxford University Press, New York, 1969).
[2]T. D. Kühne and R. Z. Khaliullin, Nat. Commun. **4**, 1450 (2013).
[3]N. J. English and J. M. D. MacElroy, J. Chem. Phys. **119**, 11806 (2003).
[4]N. J. English and J. M. D. MacElroy, J. Chem. Phys. **118**, 1589 (2003).
[5]N. J. English, Mol. Phys. **104**, 243 (2006).
[6]R. Reale, N. J. English, P. Marracino, M. Liberti, and F. Apollonio, Chem. Phys. Lett. **582**, 60 (2013).
[7]R. Reale, N. J. English, P. Marracino, M. Liberti, and F. Apollonio, Mol. Phys. **112**, 1870 (2014).
[8]M. Avena, P. Marracino, M. Liberti, F. Apollonio, and N. J. English, J. Chem. Phys. **142**, 141101 (2015).
[9]N. J. English and C. J. Waldron, Phys. Chem. Chem. Phys. **17**, 12407 (2015).
[10]N. J. English and J. M. D. MacElroy, J. Chem. Phys. **120**, 10247 (2004).
[11]C. J. Burnham and N. J. English, J. Chem. Phys. **144**, 164503 (2016), and references therein.
[12]P. Umari and A. Pasquarello, Phys. Rev. Lett. **89**, 157602 (2002).
[13]A. M. Saitta, F. Saija, and P. V. Giaquinta, Phys. Rev. Lett. **108**, 207801 (2012).
[14]A. M. Saitta and F. Saija, Proc. Natl. Acad. Sci. U. S. A. **111**, 13768 (2014).
[15]G. Cassone, P. V. Giaquinta, F. Saija, and A. M. Saitta, J. Phys. Chem. B **118**, 12717 (2014).
[16]G. Cassone, P. V. Giaquinta, F. Saija, and A. M. Saitta, J. Chem. Phys. **142**, 054502 (2015).
[17]G. Cassone, F. Creazzo, P. V. Giaquinta, F. Saija, and A. M. Saitta, Phys. Chem. Chem. Phys. **18**, 23164 (2016).
[18]M. Dion, H. Rydberg, E. Schröder, D. C. Langreth, and B. I. Lundqvist, Phys. Rev. Lett. **92**, 246401 (2004).
[19]G. Román-Pérez and J. M. Soler, Phys. Rev. Lett. **103**, 096102 (2009).
[20]J. Klimeš, D. R. Bowler, and A. Michaelides, J. Phys.: Condens. Matter **22**, 022201 (2010).
[21]J. Wang, G. Roman-Perez, J. M. Soler, E. Artacho, and M. V. Fernandez-Serra, J. Chem. Phys. **134**, 024516 (2011).
[22]C. Zhang, J. Wu, G. Galli, and F. Gygi, J. Chem. Theory Comput. **7**, 3054 (2011).
[23]F. Corsetti, E. Artacho, J. M. Soler, S. S. Alexandre, and M. V. Fernandez-Serra, J. Chem. Phys. **139**, 194502 (2013).
[24]A. Bankura, A. Karmakar, V. Carnevale, A. Chandra, and M. L. Klein, J. Phys. Chem. C **118**, 29401 (2014).
[25]N. J. English, Energies **8**, 9383 (2015).
[26]M. J. Gillan, D. Alfè, and A. Michaelides, J. Chem. Phys. **144**, 130901 (2016).
[27]T. D. Kühne, M. Krack, F. R. Mohamed, and M. Parrinello, Phys. Rev. Lett. **98**, 066401 (2007).
[28]T. D. Kuhne, M. Krack, and M. Parrinello, J. Chem. Theory Comput. **5**, 235 (2009).
[29]J. Hutter, M. Iannuzzi, F. Schiffmann, and J. VandeVondele, Wiley Interdiscip. Rev.: Comput. Mol. Sci. **4**, 15 (2014).
[30]Z. Futera and N. J. English, J. Phys. Chem. C **120**, 19603 (2016).
[31]A. Luzar and D. Chandler, "Hydrogen-bond kinetics in liquid water," Nature **379**, 55 (1996).
[32]M. P. Allen and D. J. Tildesley, *Computer Simulation of Liquids* (Oxford University Press, 1987).
[33]N. J. English, Mol. Phys. **106**, 1887 (2008).
[34]N. J. English, P. G. Kusalik, and S. Woods, J. Chem. Phys. **136**, 094508 (2012).
[35]N. J. English and J. M. D. MacElroy, Mol. Phys. **100**, 3753 (2002).
[36]C. J. Burnham and N. J. English, J. Chem. Phys. **144**, 051101 (2016).
[37]N. J. English, Mol. Phys. **103**, 1945 (2005).
[38]C. J. Burnham, D. J. Anick, P. K. Mankoo, and G. F. Reiter, J. Chem. Phys. **128**, 154519 (2008).
[39]V. Babin, G. R. Medders, and F. Paesani, J. Chem. Theory Comput. **10**, 1599 (2014).
[40]Z. Futera and N. J. English, J. Chem. Phys. **145**, 204706 (2016).
[41]J. E. Bertie and Z. Lan, Appl. Spectrosc. **50**, 1047 (1996).